The Role of Chromophore on Pulsed Laser Ablation of Biological Tissue

by

Barry Payne

B.S., University of Denver (1994)

Submitted to the Department of Mechanical Engineering
in Partial fulfillment of the requirements for the degree of

Masters of Science

at the

Massachusetts Institute of Technology

January 1997
[February 1997]

Author _____
Department of Mechanical Engineering
17 January 1997

Certified by _____
B.B. Mikic
Professor and Associate Head, Department of Mechanical Engineering
Thesis Supervisor

Accepted by _____
A.A. Sonin
Chairman, Departmental Committee on Graduate Students

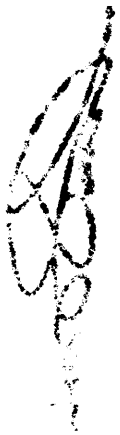

The Role of Chromophore on Pulsed Laser Ablation of Biological Tissue

by

Barry Payne

Submitted to the Department of Mechanical Engineering on January 17 1997, in
Partial fulfillment of the requirements for the degree of
Masters of Science

Abstract

Despite the widespread use of pulsed lasers in biomedical applications, the physicochemical mechanisms and dynamics of ablation processes remain unclear. The role of chromophore on pulsed infrared laser ablation of porcine dermis was investigated by performing mass removal and thermal injury experiments. A tunable Transversely Excited Atmospheric (TEA) CO_2 laser was selected for this study because it is capable of targeting both the primary chromophores in porcine dermis; tissue water and tissue structural matrix. At a wavelength of 10.6μm, the dominant chromophore is tissue water. The ablation event was consistent with explosive vaporization (spinodal decomposition) yielding a heat of ablation of 3.74×10^3 kJ/kg, an ablation threshold of 1.15 J/cm^2, and a zone of thermal injury of 53μm. At a wavelength of 9.5μm, the dominant chromophores are both tissue water and tissue structural matrix (SM). The ablation event was also consistent with explosive vaporization yielding a heat of ablation of 3.33×10^3 kJ/kg, an ablation threshold of 1.47 J/cm^2, and a zone of thermal damage of 34μm.

Under the conditions examined in this study, chromophore appears to influence ablation dynamics, but not ablation mechanism. At 9.5μm, the SM is compromised or weakened during irradiation thereby facilitating material removal, and consequently yielding a more efficient explosive ablation event with lower thermal damage. However, at 10.6μm, the SM remains intact during irradiation, inhibiting material removal, and hence causing a less efficient explosive ablation event with higher thermal damage. Ablation threshold does not seem to have any dependence on chromophore and scales with the volumetric energy density or superheat temperature within the tissue water.

Since chromophore governs the partition of energy deposition within the tissue, we hypothesize that tissue chromophore may influence ablation mechanism under different conditions.

Thesis Supervisor: B.B. Mikic
Title: Professor and Associate Head of Mechanical Engineering

Acknowledgments

Now is the time to thank those that lent a helping hand or five during my research. Dr. Nishioka and Dr. Venugopalan were responsible for starting my career in graduate research at the Wellman Laboratories of Photomedicine, and for this I am extremely grateful.

Dr. Nishioka has provided me with unlimited support and guidance throughout my time at Wellman Labs. He has taught me how to combine basic research with the reality of practical applications.

Despite 'flying the coop' Dr. Venugopalan's enthusiasm and time for this project has never faltered. Vasan has greatly influenced my development as a researcher, teaching me to think about the questions that need to be answered, and has shown me how to begin answering them.

Prof. Mikic brought his understanding and wisdom to this project. His insight will never cease to amaze me.

Andrew 'kermit' Yablon has been my friend and office mate over the last two years. He furnished me with a wealth of knowledge and laughter almost everyday! Andrew has an excellent fundamental understanding of engineering and is always willing and able to convey this to me in a clear and energetic way.

Tom Flotte assisted in the assessment of thermal damage (Chapter 3). He has taught me the subtleties of histology, and I am very grateful for his time.

The staff at Wellman Labs comprises of a multidisciplinary group who were always ready and capable to help answer questions, and encourage my research pursuits. To all of you, - a BIG thanks.

My roommates and friends have made my life outside the lab fun and crazy. They know who they are and I need not say anything more.

Lastly, a special thanks to my family. Although they are far away (green city under the sun), they are always near. Their encouragement, love and support has never diminished. This thesis is dedicated to them; Asante sana.

Contents

List of Figures

List of Tables

Glossary

Nomenclature

c - speed of light in vacuum ($m\ s^{-1}$)
c_a - speed of longitudinal wave propagation in the medium ($m\ s^{-1}$)
c_v - specific heat at constant volume ($J\ Kg^{-1}\ K^{-1}$)
e - charge of an electron (C)
E_{ion} - electron ionization energy (eV)
Fo - Fourier number (characteristic length is the absorption depth)
Fo^* - Fourier number (characteristic length is the chromophore size)
g - electron loss rate - depends on electron diffusion coefficient and spot size (s^{-1})
h_{fg} - latent heat of vaporization ($J\ Kg^{-1}$)
$Ln(x)$ - natural logarithm of x
m - mass of electron (Kg)
M - atomic mass of medium (Kg)
n_o - index of refraction
p_{sat} - saturation pressure (Pa)
t - time (s)
t_p - laser pulse duration (s)
T_{sat} - saturation temperature (K)
T_∞ - ambient temperature (K)

Greek Symbols

α - thermal diffusivity of medium ($m^2\ s^{-1}$)
δ - characteristic length considered for thermal diffusion (m)
ε_o - permittivity of free space ($F\ m^{-1}$)
ε''' - volumetric energy density deposited ($J\ m^{-3}$)
ε''_o - incident radiant exposure (time integrated heat flux) ($J\ m^{-2}$)
λ - laser wavelength (m)
μ_a - optical absorption coefficient of incident radiation within target (m^{-1})
ρ_{cr} - critical free electron density (cm^{-3})
ρ_o - initial free electron density (cm^{-3})
ρ - material density ($Kg\ m^{-3}$)
τ - momentum transfer collision time (s)
ω - frequency of radiation (s^{-1})
Ω - density of nucleation centers (m^{-3})

Chapter 1

Introduction

1.1 Background and Motivation

Pulsed lasers are widely used today in numerous medical applications because of their ability to effectively coagulate, incise and excise biological tissue. Some medical sub-specialties where lasers are used include gynecology, orthopedics, otolaryngology, and ophthalmology [13]. Despite the widespread use of lasers, the physicochemical mechanisms and dynamics of laser ablation remain poorly understood. Although modulation of laser parameters such as wavelength (λ) and pulse duration (t_p) modify the ablation process, one still cannot effectively predict biological responses to laser ablation *a priori*. Such a prediction would enable optimization of current laser applications and spark the development of the next generation medical laser systems and applications. Consequently, many investigators focus on the underlying physical and chemical mechanisms responsible for the removal of tissue using pulsed lasers.

Understanding tissue ablation poses challenges which are unique and separate from that of conventional materials such as metals and polymers for which ablation is better

understood (eg. [23, 31]). These challenges arise due to differences in composition and structure between these two classes of materials. First, unlike metals and polymers, tissue is an organic composite, composed chiefly of water and structural proteins. Since these components have different optical properties, internal energy distribution resulting from the absorption of laser irradiation can be highly heterogeneous. As these components have dramatically different mechanical properties, the structural response and dynamics of ablation are especially complex. Classical physical and chemical models are therefore inadequate to describe the behavior of tissue or the interplay between its constituents during laser tissue interactions. Second, since the ultimate tensile strength (UTS) of tissue is of the same order as its volumetric heat of vaporization, both thermal and mechanical transients arising from pulsed laser irradiation are important in the material removal process. The UTS of biological tissue is mainly governed by a structural matrix (SM) composed of extra-cellular proteins. Collagen type 1 is the primary SM protein in dermis, comprising roughly 35% by weight [28]. It follows that if the SM can somehow be compromised, the material removal process may be altered due to a change in tissue UTS. In other words, tissue constituents that absorb the laser irradiation (chromophore) and their role in preserving the tissue UTS or SM could be significant when trying to understand laser ablation as a process in general. Since metals and polymers have high tensile strength, ablation is usually mediated solely by photothermal processes.

1.1.1 Key Concepts

The basic physics of laser energy deposition is simple provided there is no light scattering within the tissue. The incident laser energy is absorbed exponentially according to Beer's Law.

$$\varepsilon(z)''' = \varepsilon_o'' \mu_a e^{-\mu_a z} \tag{1}$$

where $\varepsilon(z)'''$ is the volumetric energy density deposited, ε_o'' is the laser fluence (time integrated heat flux), z is the depth into tissue, and $1/\mu_a$ is the characteristic absorption depth. If the volumetric energy density exceeds some threshold, bulk material removal occurs.

In general, pulsed laser ablation of tissue can be mediated by three processes; photothermal, photomechanical and/or photochemical. Photothermal processes result in material removal through a phase change, such as material liquefaction and/or surface vaporization of tissue. Photomechanical processes remove material through the generation of stresses which lead to dynamic fracture. These stresses can be generated by a variety of mechanisms, including a phase change within the tissue and/or thermoelastic expansion. Photochemical processes result in decomposition through the absorption of high energy photons which can destabilize covalent bonds. Most ablation events involve

a combination of these processes, although there is no clear evidence that photochemical effects play a role in laser ablation of tissue. To better understand the interplay between mechanical and thermal processes, we introduce the concepts of *mechanical* and *thermal* confinement. These concepts relate the basic laser parameters (λ and t_p) to those material removal processes which are likely to be operative. Mechanical confinement occurs when laser energy is deposited before stresses generated by thermal expansion can traverse the heated volume. This can result in stresses which exceed the tensile strength of tissue, resulting in material removal through dynamic fracture. This process is well characterized as a photomechanical event and is often referred to as spallation [1, 25, 27]. In a one-dimensional planar geometry this occurs when the mechanical equilibration number of the heated layer is small, ie., $\tau_m \equiv \mu_a c_a t_p \leq 1$, where μ_a is the optical absorption coefficient (determined by wavelength) and c_a is the speed of longitudinal wave propagation in the medium. Tissue is thermally confined if the laser energy is deposited before the energy can diffuse through some characteristic length (δ). In a one-dimensional geometry this occurs when the Fourier number is small, ie., $Fo \equiv \alpha\delta^{-2}t_p \leq 1$, where α is the thermal diffusivity. Thermal confinement is further separated into macro-scale confinement (Fo), where the characteristic length is the tissue optical penetration depth (μ_a^{-1}), and micro-scale thermal confinement (Fo*), where the characteristic length is the chromophore size (size of tissue constituent that absorbs the laser radiation). One should note if tissue is confined on the micro-scale, it is also usually confined on the macro-scale. Furthermore,

if tissue is mechanically confined, both micro-scale and macro-scale thermal confinement is usually achieved.

The mechanism and dynamics of pulsed laser ablation for relatively long laser pulses (> 50μs) where there is no micro-scale thermal confinement is well understood as a photothermal event. This process can be modeled as rapid surface vaporization and liquid ejection [46]. However, as pulse durations decrease, these models fail because they don't consider the effects of micro-scale thermal confinement as well as laser induced stresses. If tissue is thermally confined on the micro-scale, energy transport away from the chromophore into neighboring structures is negligible, and thus selective photothermolysis of the chromophore should be considered as a potential mechanism for tissue removal [2]. In this regime where micro-scale thermal confinement but not mechanical confinement is achieved, ablation mechanisms are not well understood and in fact exhibit quite disparate ablation dynamics despite similar laser parameters. For example, UV radiation tends to remove tissue cleanly with minimal thermal damage [21, 30], whereas IR radiation tends to remove tissue more explosively with macroscopic damage and large zones of thermal injury [4]. A two part study which examined the thermodynamic responses of soft biological tissue indicated the SM and its role in preserving the structural integrity of tissue may be the reason for different ablation processes [36, 37]. The authors observed if the SM was directly targeted by choosing an appropriate wavelength (ie. 193μm, 248μm), material removal was consistent with a

process of rapid surface vaporization. However, if tissue water was instead targeted by irradiation (ie.2.79μm, 10.6μm), a slower and explosive ablation process was observed.

Although these results provide much insight into ablation processes, they are subject to debate. The experiments which led to these observations employed excimer laser radiation to target the SM of tissue. Since excimer lasers produce high energy photons (short wavelength), the contribution of optical and photochemical effects to the ablation process is unclear [3, 7, 8, 17, 33-35]. Excimer lasers are also impractical for many ablation applications since tissue removal rates may be small and they may induce mutagenic processes through DNA damage. To minimize the possibility of optical and photochemical effects, we wish to investigate the role of tissue chromophore on ablation processes by utilizing pulsed infrared lasers. IR lasers have the added advantage that they are generally cheaper and easier to maintain than UV lasers.

1.2 Research Objectives

The purpose of this thesis is to characterize ablation processes generated by pulses which create thermally confined but not mechanically confined conditions within the tissue during irradiation. We wish to relate these processes to clinically relevant parameters such as ablation efficiency, ablation threshold and extent of thermal damage. Since tissue chromophore and its role in preserving the structural integrity of tissue may be

responsible for the mechanism and dynamics of ablation, we wish to compare ablation processes when targeting the tissue SM and tissue water. The first step of this study was to choose an appropriate laser system which was capable of targeting both collagen (collagen type 1 is the primary SM protein in dermis) and water utilizing IR wavelengths (to avoid photochemical effects). The absorption spectra of dry collagen [45] and water [5] is shown in **Figure 1**. A tunable Transversely Excited Atmospheric (TEA) CO_2 laser was selected for this study since it is capable of producing wavelengths from 9-12μm with similar spatial and temporal characteristics. At 10.6μm (a common laser line) the dominant chromophore is water, while at 9.5μm, the absorption of both collagen and tissue water are roughly equal. While we authors realize other IR wavelengths such as 6.45μm may more effectively target the SM (higher absorption), such lasers lines are not broadly available [10].

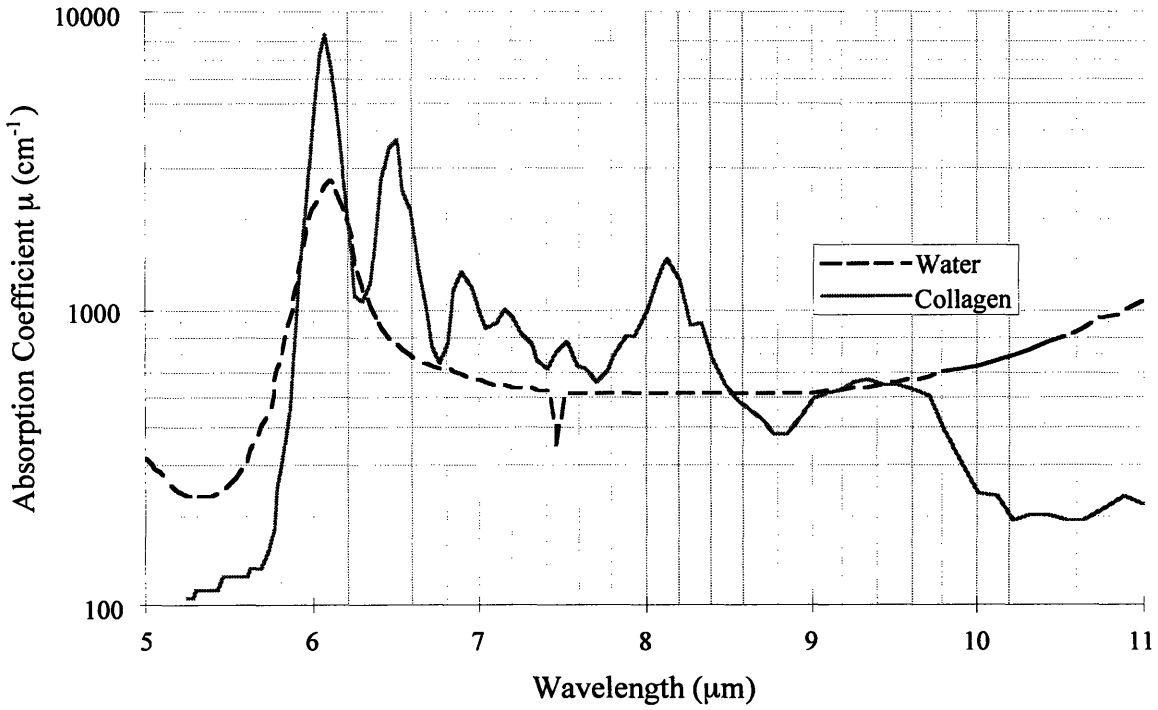

Figure 1 Absorption spectra for dry collagen and water in the far IR region.

To compare the energetics of ablation events between the two wavelengths, straight forward yet insightful experiments were performed. Although more complex dynamic experiments (eg. stress measurements, surface displacement and pump probe techniques) are possible, they rarely yield information on the parameters which are of primary clinical importance such as material removal efficiency, minimum energy density for material removal, and extent of thermal injury. However, once a thorough understanding of these clinical parameters is achieved, more complex dynamic experiments should provide useful information about the fundamental mechanisms of ablation (see Future Work, Chapter 4). As such, the specific aims of this investigation were:

1) Compare ablation efficiencies and thresholds for TEA CO_2 irradiation of porcine dermis at wavelengths 10.6μm and 9.5μm.

2) Compare the depth of residual thermal damage in porcine dermis for both wavelengths.

Chapter 2

Effect of Tissue Chromophore on Ablation Efficiency and Threshold

2.1 Introduction

Ablation threshold and efficiency are very important in most medical laser applications where removal of tissue is desired. Ablation threshold represents the minimum amount of radiant exposure (energy per unit area) needed to cause material removal. Ablation efficiency represents the incremental mass removed per unit of delivered energy. The *heat of ablation* is often referred to in the literature (eg. [40]) and is a measure of energy needed to incrementally remove a unit amount of tissue; ie. reciprocal of efficiency. Consequently, a lower heat of ablation implies a more efficient ablation process. Ablation efficiency is separate from *total efficiency*, which is total mass removed for a given energy. Total efficiency therefore depends on ablation efficiency and ablation threshold.

Ablation efficiency yields important information about ablation mechanism. To understand how ablation mechanism relates to efficiency, we examine the heat of ablation in a purely photothermal event where there is no mechanical confinement. If one assumes

a vaporization event, one would expect the heat of ablation to be close to the latent heat of vaporization of water (2.58 J/kg) since tissue is approximately 65% water. However this is rarely observed for TEA CO_2 pulsed laser ablation of tissue at 10.6μm. For instance, the heat of ablation has been shown to depend on mechanical properties of the tissue target, varying between 0.606 J/kg for weaker tissues such as liver (UTS << 0.04 MPa), and 4.27 J/kg for stronger tissues such as skin (UTS ≈ 10 MPa) [41]. Given that the thermal and optical properties for these tissues are similar, there must exist some interplay between tissue strength and mechanical transients generated during laser irradiation. One should realize that mechanical transients in this regime are separate to mechanical transients produced under conditions of mechanical confinement.

For heats of ablation lower than the latent heat of water, the implication is that ablation occurs by explosive vaporization where removal of tissue pieces occur. Explosive vaporization is considered more efficient than pure vaporization as it does not require the mass removed to be completely vaporized. Explosive material removal has been observed and photographed at a variety of wavelengths (eg. [20, 38, 42]). Since the ablation event continues to be explosive for heats of ablation above the latent heat of water [16, 41], conventional explanations of explosive material removal efficiency (as above) are not valid. The key to resolve this discrepancy is to understand where the laser energy is used. Laser energy must either contribute to vaporization and kinetic energy of ablated material or remain in the tissue. Since the kinetic energy of the ablation particles is negligible compared to total energy absorbed (≤ 2%), laser energy not consumed by the

vaporization of ejected material must remain in the tissue, causing thermal damage by heating and denaturing tissue components. It follows that efficient explosive ablation processes (low heat of ablation) should achieve minimal residual thermal damage. In other words, if a larger fraction of incident energy is used for tissue removal, a smaller fraction of incident energy is available to cause thermal damage. The question still remains as to what causes a process to be more or less efficient. If the chromophore is the tissue SM, a phase change may occur in the tissue and allow material removal through rapid surface vaporization. Efficiency will accordingly depend solely on the tissue's latent heat which is similar to water. However, if the SM remains intact during irradiation (ie. by targeting water), material removal and expansion is inhibited, and thus a slower yet more explosive ablation process may be observed. In this case efficiency should depend on the strength of tissue [41].

The onset of ablation (ablation threshold) yields additional information about ablation mechanism. In the case where mechanical confinement is not achieved, ablation threshold is probably governed by a photothermal process since negligible tissue is removed. Consequently, ablation threshold in this regime should scale with the sensible heat of water, and tissue chromophore or mechanical strength should have little effect. Previous data using 10.6μm TEA CO_2 irradiation without micro-scale thermal confinement (ie. no selective photothermolysis) showed ablation threshold to be independent of tissue type [41]. One should note however, under different conditions (eg. mechanical confinement) ablation threshold may not scale with the sensible heat of water.

There are three common ways to measure mass removal to obtain ablation efficiency and threshold. Probably the easiest method is to measure the number of pulses needed to perforate a given thickness of tissue for a range of incident fluence. The mass removed is calculated by multiplying tissue density with crater volume assuming a cylindrical crater shape. Although the assumption of crater shape is usually sound, this method suffers from variable pulse number effects. At low incident fluence, a much larger number of pulses is needed to perforate a given thickness of tissue than at high incident fluence. Since the repetition rate is generally fixed, large times are required for ablation at low fluences, which may cause the tissue target to become dehydrated. Since the absorption coefficient is usually a strong function of the tissue hydration state, mass removal will be affected. In addition, as the remaining tissue thickness decreases during ablation, the tissue becomes less optically thick (ie. incident fluence is not completely absorbed by the tissue). The second method involves measuring the crater depth and calculating the mass removed using the spot size and density of tissue. Profilometers can be used to measure the crater depth (± 5Å), however, they are only effective for measuring depths of rigid substances. For tissue, the most common method to measure crater depth is by utilizing histologic sections. Although measurements under the microscope are straight forward, many factors contribute to uncertainty. First, the crater depth is often altered during processing and second, the crater profile is not uniform which necessitates 3-D reconstruction for accurate measurements. The third method involves the measurement of

the mass before and after ablation. This method is by far the most direct and is limited only by the precision of the mass balance used and uncertainties associated with surface evaporation during the experiment. The basic concept of the mass balance setup has been previously described [39]. In this study we use this method to determine *in vitro* the mass of porcine dermis tissue removed during pulsed laser ablation of a TEA CO_2 laser. These results are compared to previous work and explained both qualitatively and quantitatively.

2.2 Materials and Methods

Sections of porcine reticular dermis (~4 mm thick) were excised immediately postmortem and were kept refrigerated and hydrated in physiologic saline (Baxter Healthcare Corp.) until use. Porcine dermis was selected for this study since it is very similar to human dermis. These sections were irradiated at 1 Hz within 12 hours with a N_2 starved TEA CO_2 laser (Lumonics 840) operating at wavelengths 10.6μm and 9.5μm. The wavelengths were selected by tuning a diffraction grating at the rear optic mirror of the laser. The diffraction grating was calibrated using a CO_2 spectrum analyzer (Laser Craft, Santa Rosa, CA). The temporal width of the laser pulse consisted of one 180ns spike (FWHM - no measurable tail) as measured by a pyroelectric detector with a response time of 500ps (Molectron Detector P5-02, Portland, OR). The output laser emission was horizontally polarized with a pulse to pulse energy variation less than 4%. Table 1 summarizes the

specific laser and tissue parameters. The optical properties are determined by modeling tissue as 65% water and 35% collagen [28].

Laser	λ [μm]	t_p [ns]	$1/\mu_a$ [μm]	τ_m (= $t_p\mu_a c$)	Fo (= $t_p\alpha\mu_a^2$)	Fo* (= $t_p\alpha/\delta^2$)
TEA CO_2	10.6	180	16.6	16.3	8.5E-05	.26-2.3E-02
TEA CO_2	9.5	180	18.3	14.8	7.0E-05	.26-2.3E-02

Table 1 Relevant laser and tissue parameters for TEA CO_2 irradiation of porcine dermis.

Prior to irradiation, 6mm biopsy punch samples (Baxter Healthcare Corp.) were obtained and placed in a Plexiglas holder on the pan of a digital balance (Mettler Instr. Corp., model AE163, Hightstown, NJ) so that all ablated material would land off the pan. The precision of the digital balance was $\pm 10\mu g$ and calibration experiments indicated that the measurement uncertainty was less than 5%. The number of pulses delivered to the tissue was fixed at 12 to insure sufficient mass removal but minimize tissue dehydration during the experiment. The mass loss data was acquired on a Macintosh LC computer at 2.4Hz using LabView (National Instruments, Austin TX) software. **Figure 2** shows the experimental setup. A 15 mm aperture was used to select a uniform portion of the laser output energy. Plastic and teflon attenuators were used to vary the incident energy that reached the tissue target. A HeNe laser coupled with a beamsplitter was used to define a fixed point in space where each tissue front surface was placed (ablation plane). A 203mm ZnSe positive lens was used to focus the laser beam energy to a spot. The spatial

profile was measured by stepping through the ablation plane with a 300μm aperture and averaging the energy using a pyroelectric detector (J3-09, Molectron Detector). Three dimensional spatial profiles are shown for wavelengths 10.6μm (**Figure 3**) and 9.5μm (**Figure 4**). The $1/e^2$ diameters were calculated using a gaussian least mean squares fit and are 2.68mm and 2.44mm for 10.6μm and 9.5μm respectively. The difference in spot sizes is due to slight differences in laser mode shape and refractive index of the ZnSe lens at 10.6μm and 9.5μm.

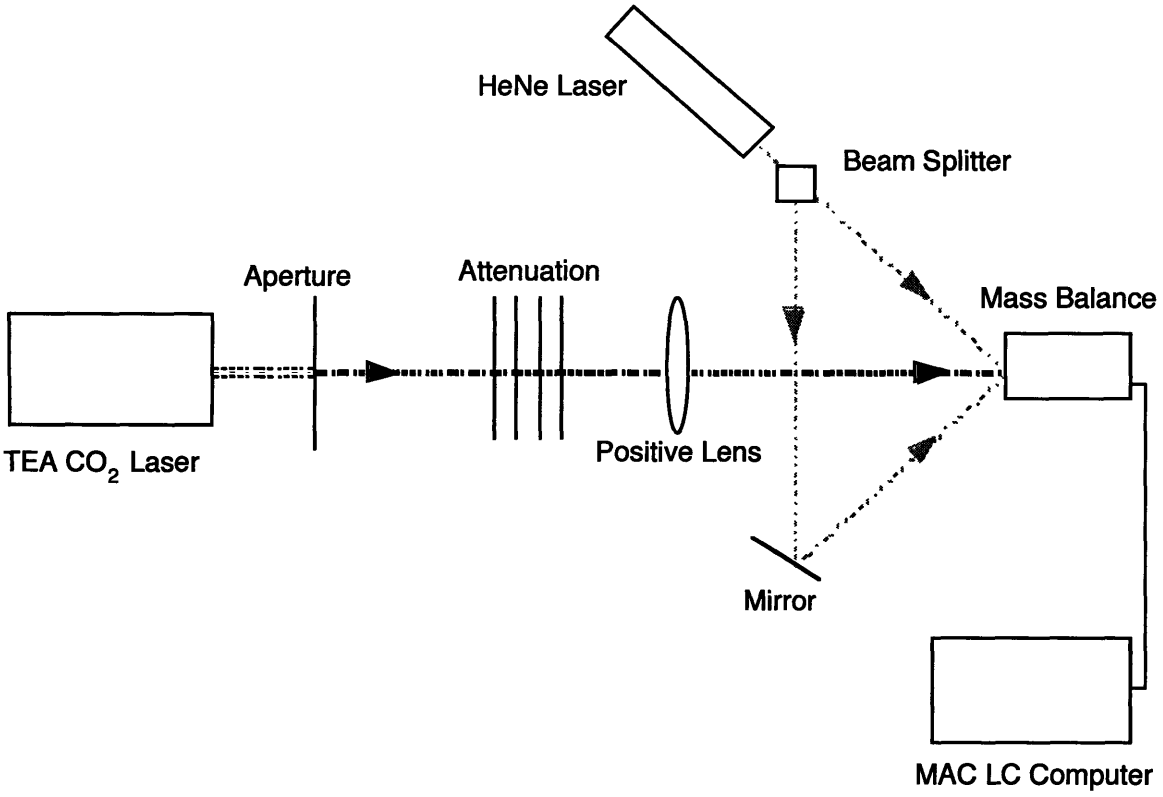

Figure 2 Mass removal experimental setup.

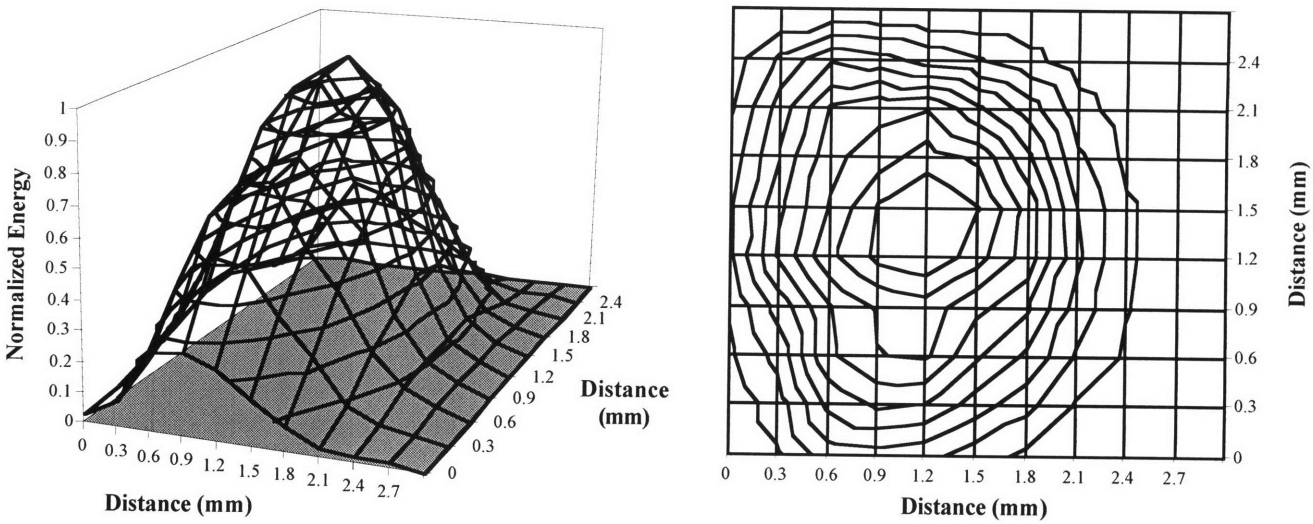

Figure 3 TEA CO_2 spatial profile at 10.6μm. Using a least mean squares fit, the diameter at $1/e^2$ intensity is found to be 2.68mm.

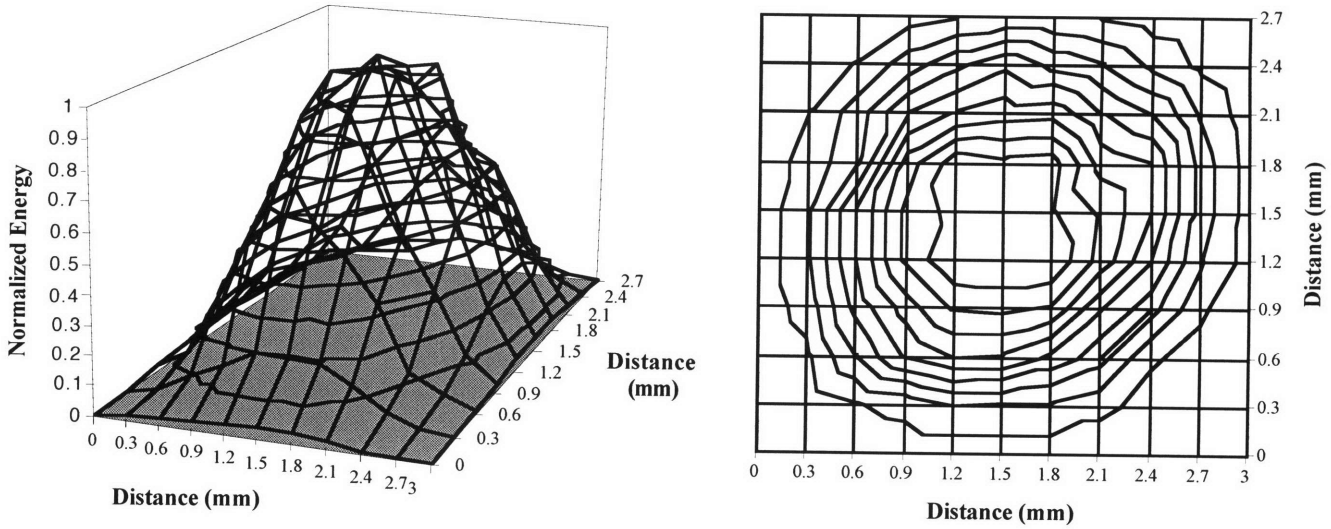

Figure 4 TEA CO_2 spatial profile at 9.5μm. Using a least mean squares fit, the diameter at $1/e^2$ intensity is found to be 2.44mm.

2.3 Results

Figure 5 shows a typical plot of the mass lost as recorded by the digital balance. Before the tissue is irradiated, mass removal is due to water evaporation from the tissue surface. Once irradiation commences, a step in mass removal rate is observed due to ablation. After irradiated is complete, mass removal continues to be caused by evaporation. A linear regression is performed on the mass loss slopes before and after ablation. The slopes agree to within 3 % of each other. The y-intercepts are calculated using the average of the slopes to yield a total corrected mass loss for the given fluence.

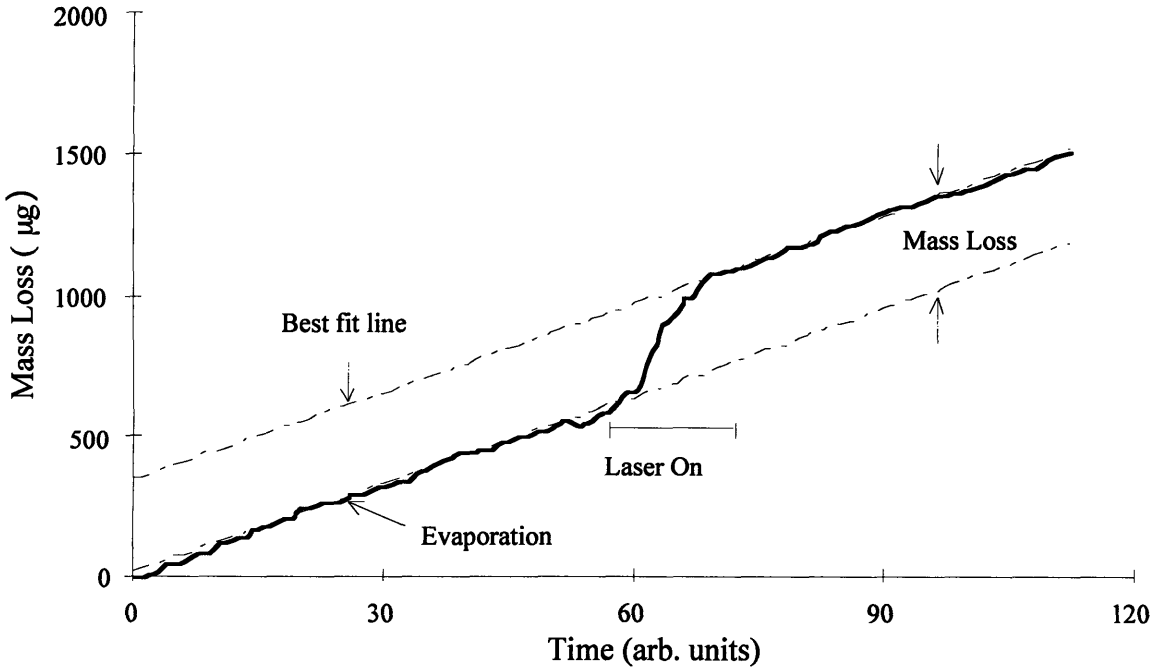

Figure 5 Typical mass loss versus time curve for TEA CO_2 irradiation. 12 pulses at 1 Hz were delivered to the porcine dermis target. Mass removal before and after the laser is turned on is due to evaporation.

The process is then repeated for different fluences and normalized over area and pulse as shown in **Figure 6.**

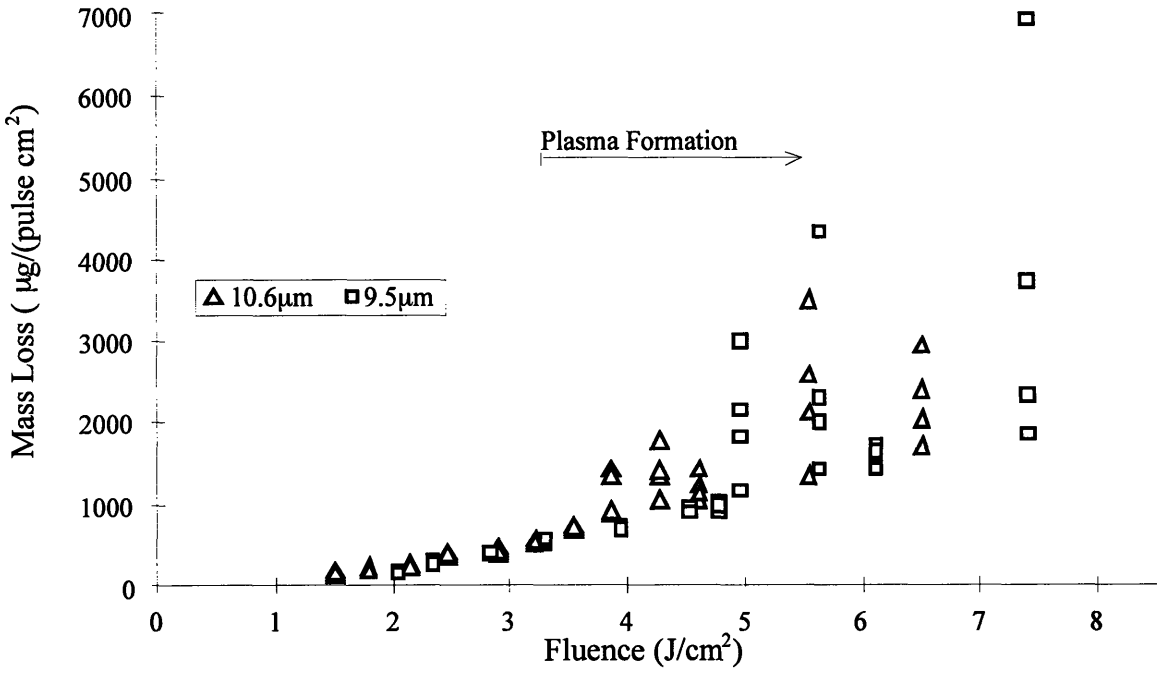

Figure 6 Mass of porcine dermis removed per pulse per area versus laser fluence by a TEA CO_2 laser at wavelengths 10.6μm and 9.5μm. The spread of the data at higher fluences is due to plasma formation.

Optical breakdown or plasma formation (visually observed as a bright white flash) caused the data to become scattered at fluences above 3.7 J/cm^2 and 5 J/cm^2 for wavelengths 10.6μm and 9.5μm respectively. A linear regression was performed on the data for fluences where optical breakdown was not observed. The resulting least squares fit is shown in **Figure 7.** A summary of the regression parameters and constants is shown in Table 2. The slopes of the regression at 10.6μm and 9.5μm differ with 90% confidence levels while the x-intercept differs with 95% confidence levels.

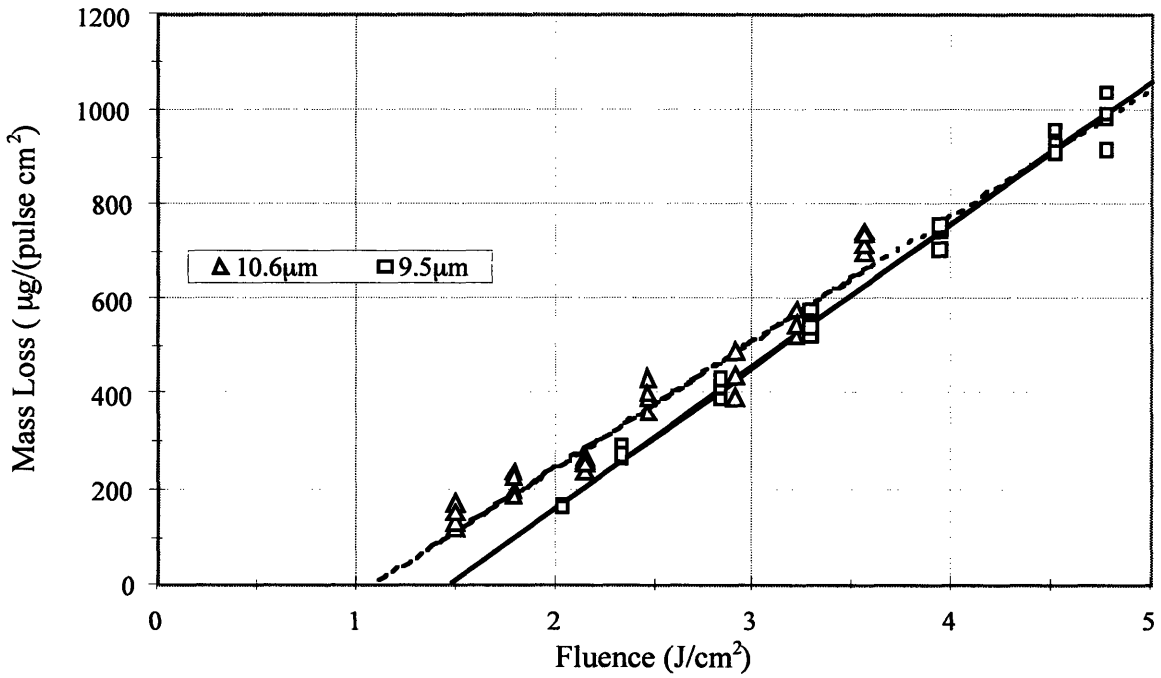

Figure 7 Mass of porcine dermis removed per pulse per area versus laser fluence by a TEA CO_2 laser. Data are fit to a linear regression before any optical breakdown was observed.

Wavelength	**10.6μm**	**9.5μm**
No. of Samples	28	28
Fluence Range	2.0-4.8 J/cm²	1.5-3.6 J/cm²
Slope	267 μg/J (242-292)[a]	300 μg/J (290-311)
Correlation Coefficient (r^2)	0.95	0.99
X-axis Intercept	1.47 J/cm² (1.41-1.54)[a]	1.15 J/cm² (1.03-1.27)

[a]95% Confidence interval

Table 2 Summary of important linear regression parameters for 10.6μm and 9.5μm for TEA CO_2 irradiation of porcine dermis.

The slope of the line denotes mass removed per energy used, which is ablation efficiency (μg/J). The x-intercept denotes the energy needed for the onset of ablation, which is ablation threshold (J/cm^2). **Table 3** summarizes the heat of ablation, ablation threshold and onset of plasma formation for wavelengths 10.6μm and 9.5μm. The ablation event at both wavelengths appeared to be explosive vaporization, causing tissue fragments to collect on and near the ZnSe focusing lens. In addition, a loud cracking noise was heard when tissue was removed.

Wavelength (μm)	Ablation Threshold (J/cm^2)	Heat of Ablation (kJ/kg) X 10^{-3}	Onset of Plasma (J/cm^2)
10.6	1.15	3.74	3.7
9.5	1.47	3.33	5.0

Table 3 Summary of important ablation parameters for wavelengths 10.6μm and 9.5μm irradiation of porcine dermis with a TEA CO_2 laser.

2.4 Discussion

There are three important observations regarding TEA CO_2 laser irradiation of porcine dermis at wavelengths 10.6μm and 9.5μm. First we consider the onset of plasma formation. Plasma formation was determined by the step increase in standard deviation of a set of mass loss data points. **Figure 6** clearly shows the marked increase in the

spread of data due to optical breakdown. Plasma was also visually observed by a bright white flash at the tissue surface which correlated well with the increased data spread. The study of plasmas is complex and only a short explanation is given here. During irradiation, water vapor at the tissue surface which is normally transparent becomes ionized (dielectric breakdown) by absorption of the incident laser light. The ionization results in a *gas* of charged particles which strongly absorbs the remaining laser energy. Consequently, rapid local heating occurs, causing the plasma to expand and produce an audible acoustic signature and visible emission . There are two mechanisms which lead to laser induced breakdown; ionization through direct multiphoton absorption, and cascade or avalanche ionization [19]. Multiphoton ionization is a non linear optical process which is usually only significant at high irradiance (short pulse durations $\leq$ 7ns) in pure mediums. Cascade ionization requires a few free electrons in the focal volume (*seed* electrons) at the beginning of the pulse. These free electrons absorb photons in a process known as inverse bremsstrahlung and may ionize molecules by collision. This generates additional free electrons which absorb more laser energy and ionize other molecules. This process continues geometrically and thus produces an electron avalanche. Optical breakdown will occur if the free electron density can reach a certain critical value (ρ_{cr}) despite losses due to diffusion, attachment, etc., within the duration of the laser pulse. For an impure medium such as tissue, initial free electrons probably come from easily ionized impurities which act as shallow donors. Since ionization occurs through thermally induced collisions, the onset of plasma formation should scale with the energy

density within the tissue water. The volumetric energy density for the onset of plasma is 3100 J/cm^3 and 2900 J/cm^3 for 10.6μm and 9.5μm wavelengths respectively and are roughly equivalent. Using a modified rate equation, one can obtain the following analytic expression for irradiance threshold corresponding to cascade (avalanche) breakdown ([19] eq. 58 and 59).

$$I_{th} = \left[\frac{C_l\left(1 + \omega^2\tau^2\right)}{\tau}\right]\left[g + \frac{2}{t_p} ln\left(\frac{\rho_{cr}}{\rho_o}\right)\right] + \frac{C_l m\omega^2}{M} \tag{2}$$

and

$$C_l = \frac{mcn_o\varepsilon_o E_{ion}}{e^2} \tag{3}$$

where m is the mass of an electron, e is the charge of an electron, M is the atomic mass of the medium, ρ_o is the initial free electron density, c is the speed of light in a vacuum, n_o is the index of refraction of the medium at frequency ω, ε_o is the permittivity of free space, E_{ion} is the electron ionization energy, τ is the momentum transfer collision time, t_p is the pulse duration and g is the electron loss rate (which depends on electron diffusion coefficient and spot size). Equation (2) yields an irradiance threshold of 1.7 × 10^7 W/cm^2 for water, which is in good agreement to experimental values of 2.0 × 10^7 W/cm^2 and 2.7 × 10^7 W/cm^2 for 10.6μm and 9.5μm wavelengths respectively. Note the breakdown threshold for 9.5μm is higher than the breakdown threshold for 10.6μm. This is because the initial free carrier density (ρ_o) comes from the ionization of impurities

caused by thermal excitation. Ionization through thermal excitation depends on temperature which depends on absorption depth. Since the absorption depth for 9.5μm is higher than for 10.6μm, more energy is required to achieve the same temperature (or volumetric energy density) and hence delay optical breakdown. In addition, it is interesting to note an increase in ablation efficiency in the regime of plasma mediated ablation. This is in contradiction to previous results where the onset of plasma caused a saturation of mass removal with increasing fluence [16, 40]. In these earlier studies however, the pulse structure consisted of an initial spike (≈100ns) and a long tail (≈1.9μs), both containing equal amounts energy. Due to the long time scale of the tail, much of the incoming energy was probably shielded by the high absorbing plasma. Hence, a lower fraction of energy actually reached the target which saturated mass removal. In our study, all the energy was contained in a single 180ns temporal spike, and thus a larger fraction of the laser energy may have reached the target before the plasma had fully formed.

Second, we observe that material removal for both wavelengths occurs by explosive vaporization, causing tissue fragments to collect on and near the ZnSe focusing lens. We had first hypothesized that by directly targeting the SM (9.5μm), we may observe a surface mediated vaporization event compared to an explosive event when the SM remains intact (10.6μm) during irradiation. It appears however, tissue chromophore has little or no effect on ablation mechanism in this regime. To reconcile these differences, we

invoke an argument which states that material removal (in this regime) is governed not by tissue chromophore, but instead volumetric power density. Volumetric power density (q_o''') represents the rate at which energy is deposited into the tissue target. For high volumetric power densities, the rate of energy consumption by the formation and growth of nucleation centers is insufficient to prevent the tissue water from becoming superheated to the spinodal limit. When the spinodal limit is reached, the superheated water becomes mechanically unstable and a rapid phase transition to vapor is forced by a process known as spinodal decomposition or flash/explosive boiling [6, 32]. At atmospheric pressure, the maximum theoretical temperature is estimated to be 305°C, whereas 280°C is the highest temperature achieved to date. The process of explosive or flash boiling for the removal of tissue has been proposed by numerous investigators [12, 24, 26], and the viability of this mechanism has been confirmed by a detailed analysis [37]. Here we present only the final equations to obtain a numerical estimate for the volumetric power density necessary to achieve flash boiling under our experimental conditions (q_{sp}'''). The incident volumetric power density necessary to achieve flash boiling when the bubble growth is controlled by the inertia of the surrounding liquid is given by:

$$q_o''' >> q_{sp}''' = \frac{4\pi\rho_v h_{fg}\Omega t_p^2}{3}\left\{\frac{2a}{3\rho_f}\left[e^{-\frac{b}{T_v}} - e^{-\frac{b}{T_{sat}}}\right]\right\}^{\frac{3}{2}} \qquad (4)$$

The incident volumetric power density neces`sary to achieve flash boiling during heat transfer controlled bubble growth is given by:

$$q_o''' >> q_{sp}''' = \frac{4\pi\rho_v h_{fg}\Omega t_p^{\frac{1}{2}}}{3}\left\{\frac{\rho_f c_f\left(T_\infty - T_{sat}\right)}{\rho_v h_{fg}}\right\}^3\left(\frac{12\alpha_f}{\pi}\right)^{\frac{3}{2}} \qquad (5)$$

In these expressions, ρ_v and T_v are the density and temperature of vapor within the bubble; ρ_f, c_f and α_f are the density, specific heat, and thermal diffusivity of the surrounding liquid; T_{sat} is the saturation temperature of the liquid; T_∞ is the temperature of the surrounding superheated liquid, h_{fg} is the latent heat of vaporization and Ω is the density of nucleation centers. For water, the saturation pressure is related to the saturation temperature through the empirical expression $p_{sat} = a \cdot \exp(-b/T_{sat})$, where $a = 3.075 \times 10^{10}$ Pa and $b = 4688.2$K [43]. The density of nucleation centers Ω is calculated by assuming the maximum volume that the vapor bubbles can occupy immediately at the end of irradiation is on the order of the heated volume, and thus $\Omega V(t_p) \approx 1$.

The volume of each nucleation site $V(t)$ during heat transfer controlled bubble growth is given by:

$$V(t) = \frac{4\pi}{3}\left\{\frac{\rho_f c_f\left(T_\infty - T_{sat}\right)}{\rho_v h_{fg}}\right\}^3 \left(\frac{12\alpha_f}{\pi}t\right)^{\frac{3}{2}} \qquad (6)$$

In our case, bubble growth occurs over a characteristic duration of $t_p \approx 400$ns. The reciprocal of $V(t = 400\text{ns})$ yields the density of nucleation centers to be $\Omega = 5 \times 10^{16}$. We can now plot q'''_{sp} versus laser pulse (t_p) as shown in **Figure 8**. Note for exposure durations less than $\approx$ 5 ns, the bubble growth is constrained by the inertia of the surrounding liquid, but for longer exposures, bubble growth is limited by heat transfer from the superheated liquid to the vapor. The value of the incident volumetric power density at ablation threshold for our TEA CO_2 laser is shown clearly above the volumetric power density necessary to achieve flash boiling.

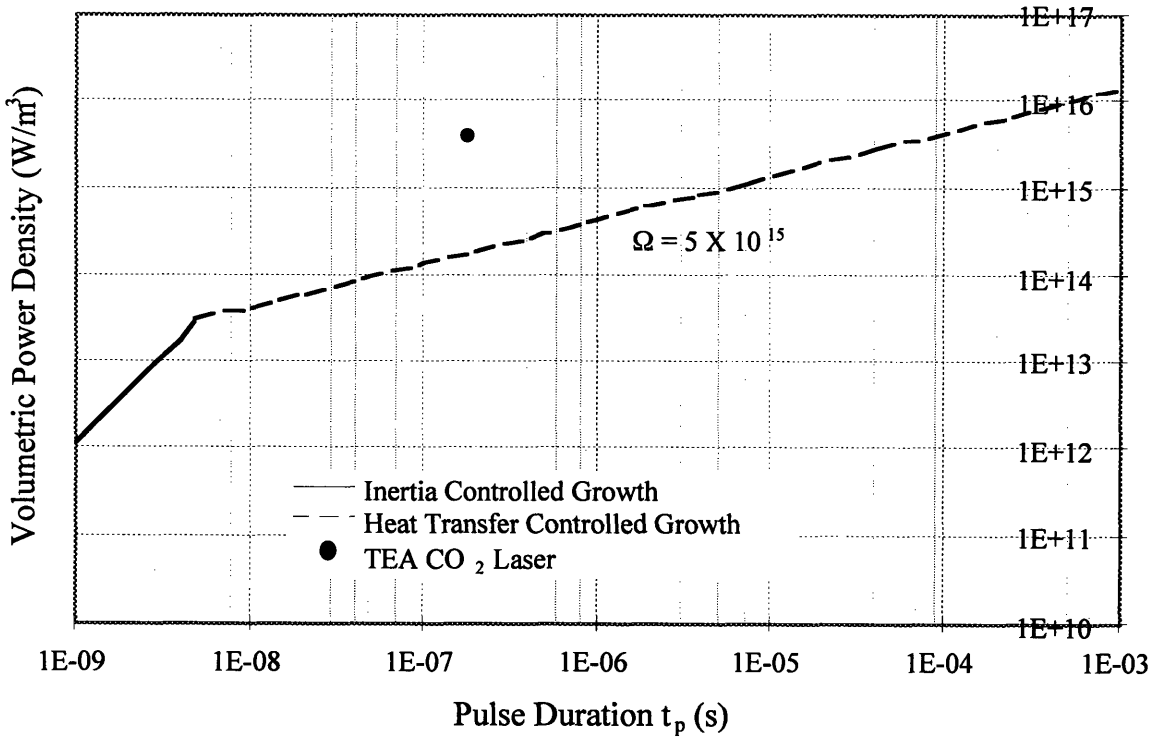

Figure 8 The solid and dashed lines represent the volumetric power density (q'''_{sp}) required to achieve flash boiling of tissue water versus laser pulse duration. The number density of nucleation sites Ω is a free parameter. The data point (•) represents the volumetric power density achieved at ablation threshold for the TEA CO_2 laser at 10.6μm and 9.5μm.

We must also check the temperature of the liquid water at ablation threshold to ensure the radiant exposure is sufficient to achieve superheating to the spinodal limit. The change in temperature at the tissue surface is given by:

$$\Delta T = \frac{\mu_{H_2O}\varepsilon''_o}{\rho_{H_2O}c_{v,H_2O}} \tag{7}$$

Where ε''_o is the threshold fluence and μ_{H20}, $c_{v,H20}$, ρ_{H20}, are the absorption coefficient, specific heat at constant volume and density of water. Using this equation we find the

surface temperature at ablation threshold to be 230°C and 258°C for 10.6μm and 9.5μm respectively. Both values of ΔT are sufficient to heat the tissue water near the spinodal limit, causing explosive boiling.

Although tissue chromophore appears to have little or no effect on ablation mechanism, it may however affect ablation dynamics. After the tissue water has reached the spinodal limit, phase separation occurs generating very high pressures approaching the saturation pressure. At 305°C the saturation pressure for water is ≈ 9 MPa which is of the same order as the ultimate tensile strength (UTS) of porcine dermis; σ_{UTS} ≈ 8-10 MPa [44]. It follows that tissues with weakened mechanical strength (UTS) will be less likely to impede material removal, thereby resulting in a more efficient ablation event. In other words, when phase separation occurs, the ease or efficiency of material removal will directly depend on the tissue UTS. These observations appear to be consistent with our results and also those of Walsh and co-workers who observed increased ablation efficiencies for mechanically weaker tissues [41]. At 10.6μm, water is the dominant chromophore and thus the SM remains intact during irradiation, causing a less efficient ablation process or higher heat of ablation. However, at 9.5μm the SM is compromised or weakened during irradiation thereby facilitating material removal, and consequently yielding a more efficient ablation event or lower heat of ablation (see **Table 3**). Unfortunately, the heat of ablation for 10.6μm and 9.5μm only differ within 90% confidence levels, although repeated experiments exhibit the same trend. The reason for

this small difference is presumably because we do not effectively target the SM. At 9.5μm the tissue SM is not sufficiently weakened because only one third of the laser energy by volume is absorbed by the SM. Since the dynamics of phase separation in a composite structure is very complicated, one must be careful when modeling ablation processes in this regime and consequently simple ablation models derived from Beers law may be misleading .

Third, we consider the onset of ablation or ablation threshold. We have already established the ablation mechanism to be consistent with explosive vaporization (spinodal decomposition) in this regime. Accordingly, the onset of ablation must be governed by the superheat nature of the tissue water and be independent of tissue SM. In other words, the onset of ablation is triggered by spinodal decomposition, and hence tissue mechanical integrity has little influence. If our hypothesis is correct, the energy per unit volume within the tissue water at threshold must be the same for both 10.6μm and 9.5μm wavelengths (note this is equivalent to comparing superheat temperatures in the tissue water at threshold). The energy per unit volume or volumetric energy density in the tissue water for 10.6μm and 9.5μm are 693 J/cm^3 and 803 J/cm^3 respectively representing a 14.7% difference. Although these results appear to be consistent with other CO_2 data [37, 40], large discrepancies are observed when comparing threshold volumetric energy densities at other wavelengths. For example, the threshold volumetric energy density for Er:YSGG is only 400 J/cm^3 [37]. The authors accounted for this difference by arguing

that the maximum local threshold fluence for Er:YSGG is twice the average value since the beam spatial mode is gaussian. While this is true in their case, similar arguments could be made for our TEA CO_2 spatial profile. In our experiments a flat top spatial profile was focused down to the target using a ZnSe lens. The resulting spatial profile at the focus should therefore be a sinc function [18]. Since the experiment was not performed at the focus, the spatial profile is somewhat altered (**Figure 3 and Figure 4**), although the maximum local fluence is still much higher than the average fluence used in our calculations. These arguments illustrate how misleading it is to compare results with other investigators. Although similar lasers and wavelengths may have been used, the pulse duration used in the experiments varied by almost two orders of magnitude which must modify the ablation process. Further, separate measurement techniques were used to determine ablation threshold, which is tantamount to using different threshold definitions.

Chapter 3

Effect of Tissue Chromophore on Thermal Damage

3.1 Introduction

The extent of thermal damage produced from laser ablation is important in numerous medical applications. Some applications such as photorefractive keratectomy require very little residual damage ($\approx$ 0.5μm), while other applications such as skin resurfacing require larger zones of thermal damage ($\approx$ 80μm) to provide for haemostasis [14, 30]. Thermal damage is caused by thermal energy diffusing into the tissue and denaturing tissue proteins. In IR ablation, thermal damage of collagen exhibits as many as three distinct zones. The inner most zone (surface of crater) consists of a carbonized zone often referred to as char and usually occurs for higher laser powers. The second zone is a vaculation zone. This zone is normally larger than the carbonized zone and is associated with a loss of fibrillar appearance in the collagen. The last zone consists of altered collagen fibrils that appear thicker than normal and is often referred to as a sub-boiling coagulation zone. This zone normally comprises the bulk of thermal damage [22].

There are numerous factors which affect thermal damage. First there are geometric issues such as aspect ratio. High aspect ratios mean the depth of the ablation crater is large compared to the area of irradiation. In this case, ablated material may have difficulty escaping, and consequently remains trapped at the bottom of the crater causing excess thermal damage. Second, there are issues regarding confinement. If the ablation event is mechanically confined, the production of laser induced stresses which exceed the yield strength of tissue aid in the removal of tissue constituents through dynamic fracture. In this case, the temperature in the tissue remains low, minimizing thermal damage. This process is often referred to as cold ablation. If the ablation event is thermally confined, there is negligible energy transport away from the heated volume via diffusion during irradiation, thereby minimizing thermal damage. Finally, the extent of thermal damage must also scale with absorption depth since energy deposition is exponential.

Despite a reasonable understanding of factors which influence thermal damage, it remains difficult to predict the extent of damage given a particular set of laser parameters. This is especially true when comparing short pulsed UV and IR ablation. For example, thermal damage zones for KrF-excimer laser irradiation (248nm) is an order of magnitude lower then damage zones of TEA CO_2 irradiation [4, 21, 30] despite comparable absorption depth and pulse duration. Although this discrepancy may be attributed in part to degree of mechanical confinement (ie. cold ablation for KrF), dynamic optical properties and photochemical affects, it is more likely due to a difference in energy partition. UV

radiation directly targets the tissue SM and tissue removal is consistent with a rapid surface vaporization model whereas IR radiation targets the tissue water and tissue removal is consistent with an explosive model [36, 37]. Albeit we previously stated chromophore has little influence of ablation mechanism in this regime (micro-scale thermal confinement, no mechanical confinement), we must reevaluate our definition. If the SM and tissue water is targeted with high power, the tissue water becomes superheated causing explosive vaporization. In this case chromophore only affects the dynamics of ablation and not mechanism. If one solely targets the SM however, the tissue water does not superheat and consequently surface vaporization and not explosive vaporization may occur. In other words, chromophore will influence ablation mechanism if laser energy absorbed by the tissue water is insufficient to cause superheating to the spinodal limit. In our experiments with TEA CO_2 irradiation, we have already established the ablation process to be explosive vaporization for both wavelengths caused by superheating of tissue water. In this regime, chromophore appears to affect the dynamics but not mechanism of ablation. Consequently, thermal damage should scale inversely to ablation efficiency.

There are numerous ways to quantify thermal damage including elaborate procedures such as transmission and scanning electron microscopy. We will use a technique called hematoxylin and eosin staining (H&E). This method is simple and yields sufficient information, although one must be careful in assessing thermal damage in histological slides due to various artifacts of processing. For instance, tissue often shrinks during

processing and density gradients may cause thermally altered tissue to be ejected while histologic cuts are being made. Nonetheless, one can eliminate most of these problems by comparing experiments performed on similar tissue samples processed in the same way. In this study we use hematoxylin and eosin staining to compare the zones of thermal damage *in vitro* for TEA CO_2 irradiation of porcine dermis at wavelengths 10.6μm (primary chromophore is water) and 9.5μm (chromophore is both the SM and water).

3.2 Materials and Methods

The experimental setup is identical to the ablation efficiency setup in section 2.2 (**Figure 2**), except a digital balance and computer are no longer used. The energy delivered to the tissue target was chosen based on two criteria; first, the energy was normalized with respect to ablation threshold measured in the previous experiments and second, the energy was as high as possible without causing the onset of plasma formation. The resulting fluence at the target was 3.5 J/cm^2 and 4.47 J/cm^2 for 10.6μm and 9.5μm respectively. Fifteen samples of tissue were used at each wavelength and the number of pulses delivered to each sample was fixed at 12 (other experiments which slightly varied energy and number of pulses exhibited no significant variance in thermal damage [29]). **Figure 9** illustrates the setup and procedure for histology and assessment of thermal damage. After laser irradiation, the tissue samples were fixed in formalin, set in paraffin,

cut into sections 15μm thick and stained with hematoxylin and eosin (H&E stain). The amount of thermal damage was assessed by a pathologist (the pathologist was blinded to the laser parameters used to produce the samples) using a calibrated reticle at the center of the bottom surface of each crater to eliminate edge effects. The H&E stain allowed differentiation between normal and thermally altered tissue under the microscope.

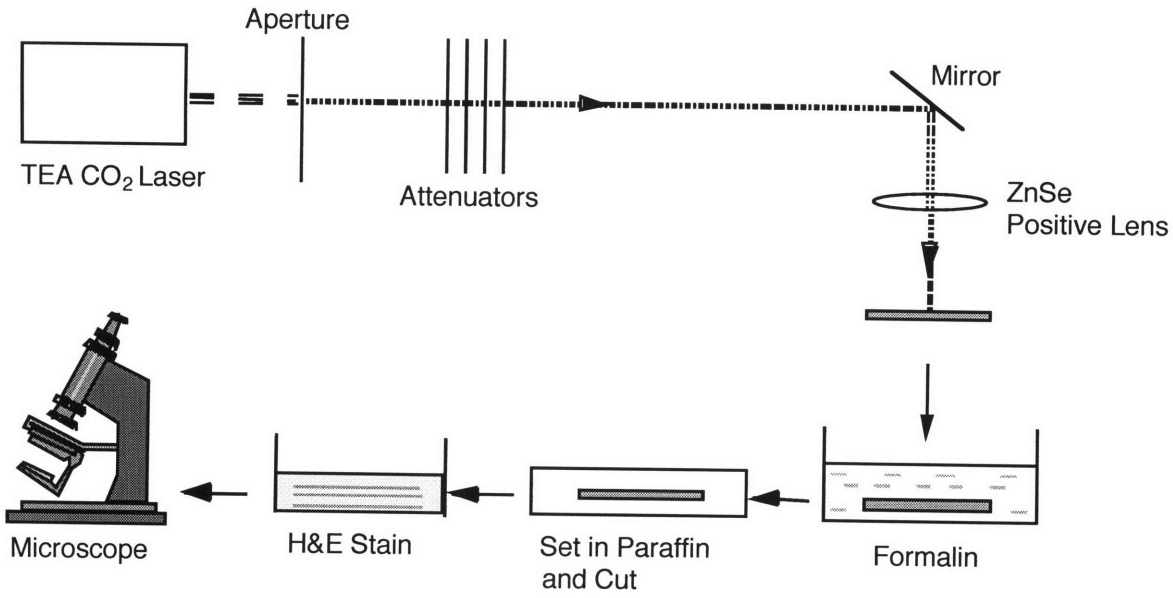

Figure 9 Illustration of histology and assessment of thermal damage procedure.

3.3 Results

Typical examples of histological sections are shown in **Figure 10**. The variance in staining clearly contrasts the difference between normal and thermally altered tissue. At 9.5μm, where the dominant chromophores are the SM and tissue water, the amount of thermal damage seems more superficial and the crater surface smooth compared to 10.6μm where the dominant chromophore is tissue water. One should recognize however, that each histological section may contain various levels of thermal damage and must therefore consistently distinguish between legitimate levels of thermal damage and levels of thermal damage due to artifacts of processing. **Figure 11** summarizes the measured levels of thermal damage. The average thickness of thermal damage was 53μm and 34μm with a standard deviation (STD) of 17μm and 9μm (P value = 0.0017) for TEA CO_2 irradiation at wavelengths 10.6μm and 9.5μm respectively.

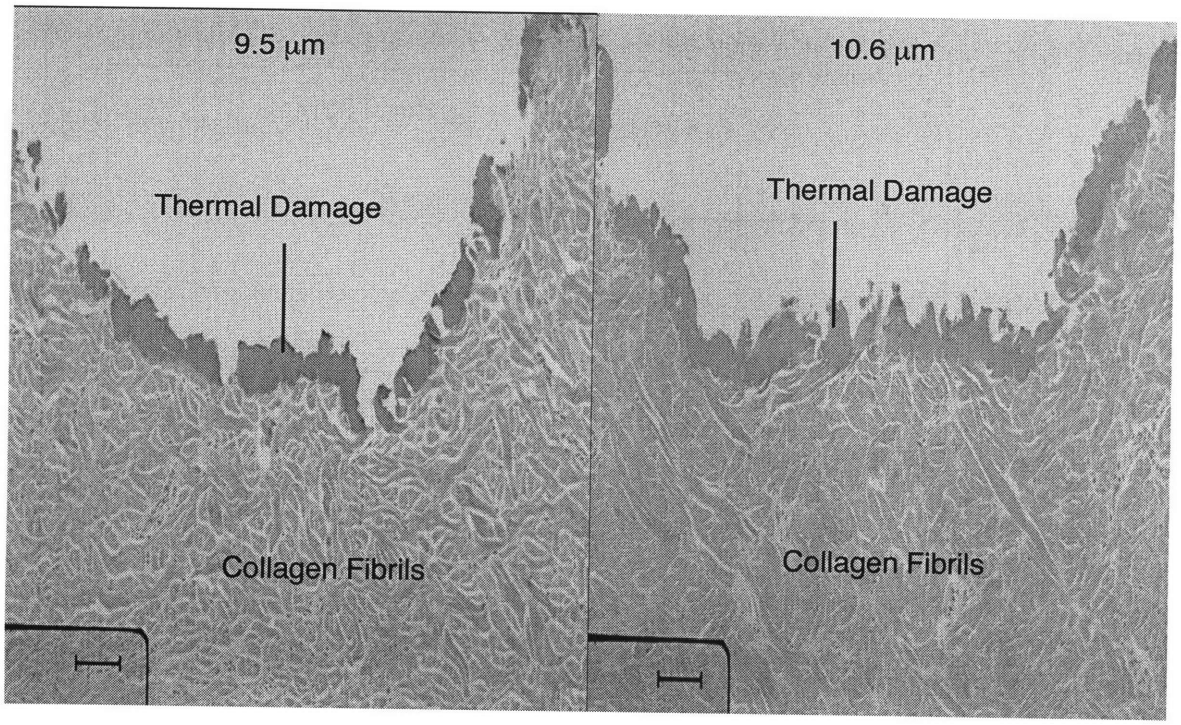

Figure 10 Example of histology slides after TEA CO_2 irradiation at wavelengths 10.6μm and 9.5μm. The length scale of the bar is 50μm long.

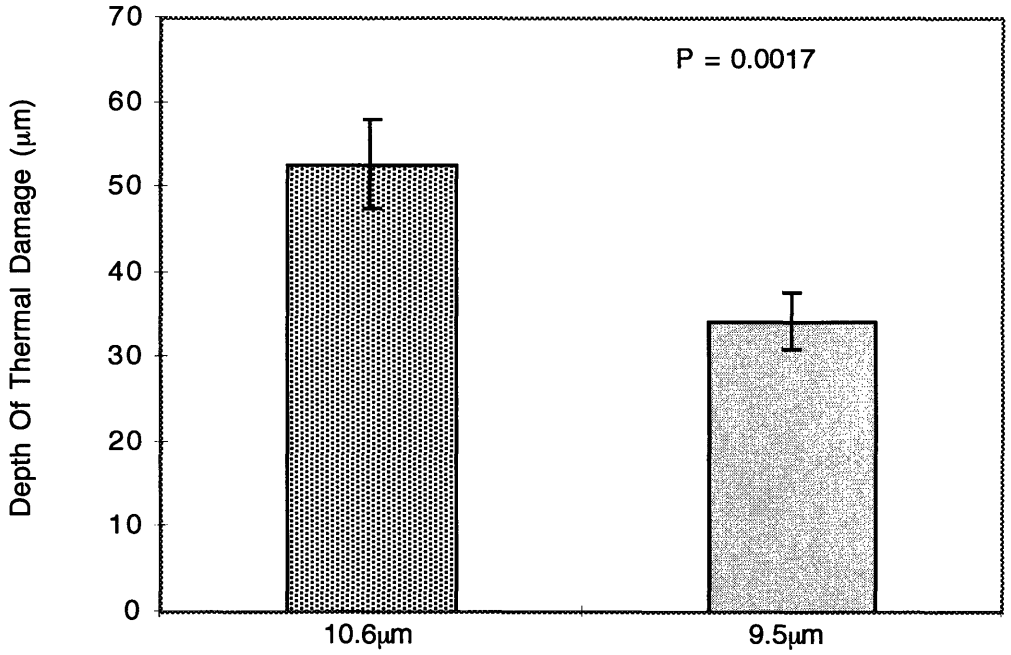

Figure 11 Summary of the measured thickness of thermal damage at wavelengths 10.6μm and 9.5μm for TEA CO_2 laser irradiation of porcine dermis. The error bars represent one standard deviation. The P value is calculated using a two-sample paired t-test assuming equal variances.

3.4 Discussion

Zones of thermal damage have been quantified for TEA CO_2 irradiation at wavelengths 10.6μm and 9.5μm. The results statistically show that thermal damage at 9.5μm irradiation is lower then for 10.6μm irradiation. This observation is consistent with our hypothesis that thermal damage is inversely related to ablation efficiency when ablation mechanism is the same. At 10.6μm, water is the dominant chromophore and thus the SM

remains intact during irradiation, inhibiting material removal and causing more thermal damage. However, at 9.5μm, the SM is compromised or weakened during irradiation thereby facilitating material removal, and consequently yielding a more efficient ablation event with lower thermal damage. Since the ratio of thermal damage is different to the ratio of ablation efficiency (≈ 32%), the inverse relationship is not linear and may depend on the relative specific heats of tissue water and collagen.

In this regime (micro-scale thermal confinement, no mechanical confinement), tissue chromophore and its role in preserving tissue UTS appears to affect ablation dynamics which influences efficiency and level of thermal damage. One should note however, that while thermal damage should decrease if the SM is more effectively targeted (efficiency should increase), there exists a threshold where ablation mechanism will change from explosive vaporization to surface vaporization, since the tissue water will no longer reach the spinodal limit. Once this occurs, the dependence of thermal damage to efficiency and chromophore is unclear, although in general, surface mediated ablation appears to exhibit lower thermal damage and higher efficiencies [11, 21, 30, 36]. This is presumably because surface vaporization does not leave a significant amount of superheated liquid within the tissue.

The observation that one can abate thermal damage with no change in ablation mechanism has significant impact for a variety of medical applications. For example, CO_2 laser burn

debridement and skin re-surfacing require ≈ 80μm of thermal damage to cause haemostasis, however current systems often leave ≈ 160μm (eg.[15]) of thermal damage, usually resulting in delayed healing. One could therefore benefit considerably by simply altering the wavelength of current systems through the utilization of a diffraction grating.

Chapter 4

Conclusions and Future Work

4.1 Introduction

Short pulsed laser ablation of biological tissue is complex. Although there are only two laser parameters (t_p, λ) which primarily govern ablation processes, they are so intricately woven together that it is difficult to extract their individual contributions. Carefully performed experiments, data analysis and interpretation have come a long way in solving the ablation puzzle. For instance, ablation through dynamic fracture (spallation) is caused when the mechanical equilibration time (τ_m) of the heated layer is less than or equal to 1. The mechanical equilibration time is proportional to pulse duration (t_p) and absorption coefficient (μ_a) which directly depends on laser wavelength (λ). Ablation mediated by surface vaporization and liquid ejection are often caused by long pulse durations (t_p), and are independent of wavelength since thermal diffusion within the tissue volume is allowed. However, the relationship between λ and t_p is unclear when ablation is caused by explosive vaporization. Moreover, the transitions between surface vaporization, explosive vaporization and spallation remain obscure. Most of these difficulties arise due to the unique composition of tissue and its properties.

In our investigations, we have tried to elucidate ablation processes in the transitional regime between explosive vaporization and surface vaporization by examining the role of tissue chromophore under conditions where micro-scale thermal confinement but not mechanical confinement was achieved. To minimize possible photochemical effects and dynamic changes in optical properties, we utilized IR irradiation (low photon energies). We used wavelengths which would target one or both of the primary chromophores in dermis; tissue water and collagen fibrils (SM). We performed ablation efficiency/threshold and thermal damage experiments since these parameters are important for most medical applications.

The format of this chapter is as follows. First the experimental results will be summarized and their implications explored with respect to ablation mechanism, ablation dynamics and practical significance. Second, some useful experiments are suggested which may illuminate additional details of ablation transitions and processes and aid in the development of physical models.

4.2 Summary of Results

The experiments were carried out on porcine dermis using a TEA CO_2 laser at wavelengths 10.6μm, where the chromophore is tissue water, and 9.5μm where the chromophore is both the SM and tissue water. At 10.6μm the ablation event was observed to be explosive vaporization yielding a heat of ablation of 3.74×10^3 kJ/kg, a threshold of 1.15J/cm^2, and a zone of thermal injury of 53μm. At 9.5μm the ablation event was also observed to be explosive vaporization yielding a heat of ablation of 3.33×10^3 kJ/kg, a threshold of 1.47J/cm^2, and a zone of thermal damage of 34μm. When the tissue SM and water are targeted (9.5μm), both heat of ablation and resulting zone of thermal damage is lower than when only the tissue water is targeted (10.6μm). Ablation threshold however, does not seem to have any dependence on chromophore and scales with the volumetric energy density within the tissue water.

4.3 Chromophore and Ablation Mechanism

In our experiments, the ablation event was consistent with a process called spinodal decomposition or explosive vaporization. In review; when the rate of energy consumption by the formation and growth of nucleation centers is insufficient to prevent the tissue water from becoming superheated to the spinodal limit, a rapid phase transition to vapor is forced in a process called spinodal decomposition or explosive vaporization.

Consequently, the rate of energy deposition (power density) in the tissue water appears to control ablation mechanism under the experimental conditions. It follows that if the SM is more effectively targeted, the volumetric power deposition within the tissue water may no longer cause superheating to the spinodal limit, and the ablation process may no longer be explosive. In other words, chromophore governs the partition of energy deposition within the tissue and accordingly may influence ablation mechanism. Therefore, tissue chromophore, or more precisely, the ratio of absorption coefficients of the chromophores within the tissue volume should govern ablation mechanism. This is presumably why UV irradiation is consistent with a process of rapid surface vaporization and not explosive vaporization [36].

In addition, it is worthwhile calculating the approximate pulse duration necessary to cause explosive vaporization. Using equation (5) and assuming volumetric energy density at threshold to be constant (ie. ablation threshold is governed by the superheat nature of the tissue water), we find the pulse duration to be $t_{sp} \approx 1\mu s$. This approximation depends on the assumed density of nucleation centers (t_{sp} = constant $\times \Omega^{-2/3}$) and therefore may not be very accurate. However, since t_{sp} is on the same order as the micro-scale thermal confinement time ($\approx 1\mu s$), the degree of micro-scale thermal confinement (Fo*) may be a good indicator of ablation mechanism.

4.4 Chromophore and Ablation Dynamics

Explosive vaporization is caused by high stresses within the heated tissue volume that are produced by phase separation of unstable superheated liquid. Consequently, the dynamics of phase separation and ablation must depend on tissue UTS. It follows that tissue with high UTS would tend to constrain phase separation and inhibit tissue removal. Since the UTS may be weakened by irradiating the tissue SM, one can presumably alter the dynamics of the ablation process by simply changing the incident wavelength. Therefore tissue chromophore and its role in preserving the UTS of tissue should influence ablation dynamics.

4.5 Practical Significance

In our experiments, we found chromophore to influence parameters such as efficiency and zone of thermal damage, which are of principal importance for many medical applications. We observed an increase in efficiency and decrease in thermal damage by changing the incident wavelength from 10.6μm to 9.5μm. The mechanism of ablation however, remained unchanged. This observation has notable impact for medical applications where it is advantageous to moderate thermal damage without changing ablation mechanism.

As suggested in (4.3), chromophore may also influence ablation mechanism, possibly affecting efficiency, threshold and zone of thermal damage. For instance, previous studies have indicated high efficiencies and low zones of thermal injury for ablation events consistent with surface vaporization [11, 21, 30, 36]. However, the specific role of ablation mechanism on such parameters remains uncertain. In addition, when small changes in efficiency or thermal damage are desired, it may not be favorable to alter ablation mechanism, since these changes could be large.

4.6 Future Work

Two main directions should be considered for further understanding of ablation processes generated by thermally confined but not mechanically confined pulsed laser ablation of biological tissue. First, experiments should be performed through the regime between explosive vaporization and surface vaporization. This may be achieved by fixing wavelength (λ) and varying pulse duration (t_p). As the pulse duration increases, one would directly observe the transition from explosive vaporization (micro-scale thermal confinement) to surface vaporization (may no longer be thermally confined). In addition, one could fix pulse duration and vary wavelength. As more energy is absorbed by the SM and less energy is absorbed by the tissue water, one should observe another transition from explosive to surface vaporization. The free-electron laser may be capable of accessing the relevant pulse duration and wavelength in the IR to perform such

experiments [9]. Second, albeit a thorough understanding of important clinical parameters such as ablation efficiency, threshold and depth of thermal damage generates insight into the fundamentals of ablation, they yield no dynamic information. In order to understand ablation as a process rather than an effect, it is necessary to perform time-resolved experiments in the transitional regime. Measurement of stress transients, surface temperature and surface displacement are techniques which should be employed.

Bibliography

1. Albagli, D., L.T. Perelman, G.S. Janes, C. von Rosenberg, I. Itzkan, and M.S. Feld, *Inertially Confined Ablation of Biological Tissue.* Lasers in the Life Sciences, 1994. **6**(1): p. 55-68.
2. Anderson, R.R. and J.A. Parrish, *Selective Photothermolysis: Precise Microsurgery by Selective Absorption of Pulsed Radiation.* Science, 1983. **220**: p. 524-527.
3. Cummings, J.P. and J.T. Walsh, Jr., *Erbium Laser Ablation: The effect of Dynamic Optical Properties.* Applied Physics Letters, 1993. **62**(16): p. 1988-1990.
4. Cummings, J.P. and J.T. Walsh, Jr., *Tissue tearing caused by pulsed laser-induced ablation pressure.* Applied Optics, 1993. **32**(4): p. 494-503.
5. Downing, H.D. and D. Williams, *Optical Constants of Water in the Infrared.* Journal of Geophys. Res., 1975. **80**: p. 1656-1661.
6. Eberhart, J.G. and H.C. Schnyders, *Application on the Mechanical Stability Condition to the Prediction of the Limit of Superheat for Normal Alkanes, Ether, and Water.* Journal of Physics and Chemistry, 1973. **77**: p. 2730-2736.
7. Ediger, M.N., G.H. Pettit, and D.W. Hahn, *Enhanced ArF Laser Absorption in a Collagen Target Under Ablative Conditions.* Lasers in Surgery and Medicine, 1994. **15**: p. 107-111.
8. Ediger, M.N., G.H. Pettit, R.P. Weiblinger, and C.C. H., *Transmission of Corneal Collagen During ArF Excimer Laser Ablation.* Lasers in Surgery and Medicine, 1993. **13**: p. 204-210.
9. Edwards, G., *Biomedical Applications of Free-Electron Lasers.* Optical Engineering, 1993. **32**(2): p. 314-319.
10. Edwards, G., *Biomedical and Potential Applications for Pulsed Lasers operating near 6.45um.* Optical Engineering, 1995. **34**(may): p. 1524-1525.
11. Edwards, G., R. Logan, M. Copeland, L. Reinisch, J. Davidson, B. Johnson, *et al.*, *Tissue ablation by a free-electron laser tuned to the amide II band.* Nature, 1994. **371**(29): p. 416-19.
12. Esenaliev, R.O., A.A. Oraevsky, and V.S. Letokhov, *Laser Ablation of Atherosclerotic Blood Vessel Tissue under various Irradiation Conditions.* IEEE Transactions of Biomedical Engineering, 1989. **36**: p. 1188-1194.
13. Gibson, K.F. and W.G. Kernohan, *Lasers in Medicine.* Journal of Medical Engineering and Technology, 1993. **17**(2): p. 51-57.
14. Green, H.A., E. Burd, and N. Nishioka, *Middermal Wound Healing.* Archives of Dermatology, 1992. **128**(5): p. 639-45.
15. Green, H.A., E. Burd, N. Nishioka, and C.C. Compton, *Skin Graft Take and Healing Following 193nm Excimer, Continuous-Wave Carbon Dioxide , Pulsed C02, or Pulsed Holmium:YAG Laser Ablation of the Graft Bed.* Archives of Dermatology, 1993. **129**(8): p. 979-88.

16. Green, H.A., Y. Domankevitz, and N. Nishioka, *Pulsed Carbon Dioxide Laser Ablation of Burned Skin: In Vitro and In Vivo Analysis.* Lasers in Surgery and Medicine, 1990. **10**: p. 476-484.
17. Hahn, D.W., M.N. Ediger, and G.H. Pettit, *Dynamics of Ablation Plume Particles Generated During Excimer Laser Corneal Ablation.* Lasers in Surgery and Medicine, 1995. **16**: p. 384-9.
18. Hecht, E., *Optics*. 2 ed. 1990, Reading: Addision-Wesley. 676.
19. Kennedy, P.K., *A First-Order Model for Computation of Laser-Induced Breakdown Thresholds in Ocular and Aqueous Media: Part 1-Theory.* IEEE Journal of Quantum Electronics, 1995. **31**(12): p. 2241-2249.
20. Koo, J.C., *Laser-Induced Explosion of Solid Material.* Journal of Applied Physics, 1977. **48**: p. 618-650.
21. Lane, R.J., J.J. Wynne, A. Torres, and R.G. Geronemus, *Ultraviolet-Laser Ablation of Skin.* Arch. Dermatol., 1985. **121**: p. 609-617.
22. McKenzie, A.L., *Physics of Thermal Processes in Laser-tissue Interaction.* Phys. Med. Biol., 1990. **35**(9): p. 1175-1209.
23. Miller, J.C. and J.R.F. Haglund, eds. *Lecture Notes in Physics*. Laser Ablation: Mechanisms and Applications. Vol. 389. 1991, Springer-Verlag: Oak Ridge, Tennessee. 362.
24. Miotello, A. and R. Kelly, *Critical Assessment of Thermal Models for Laser Sputtering at High Fluences.* Applied Physics Letters, 1995. **67**(24): p. 3535-3537.
25. Oraevsky, A.A., R.O. Esenaliev, and V.S. Letokhov, *Laser Ablation - Mechanisms and Applications*. Lecture Notes in Physics, ed. J.C. Miller and R.F. Haglund, Jr. 1991, New York: Springer Verlag.
26. Oraevsky, A.A., R.O. Esenaliev, and V.S. Letokhov, *Temporal Characteristics and Mechanism of Atherosclerotic Tissue Ablation by Nanosecond and Picosecond Pulses.* Lasers in the Life Sciences, 1992. **5**: p. 75-93.
27. Paltauf, G. and H. Schmidt-Kloiber, *Model Study to Investigate the Contribution of Spallation to Pulsed Laser Ablation of Tissue.* Lasers in Surgery and Medicine, 1995. **16**: p. 277-87.
28. Parry, D.A.D. and A.S. Craig, *Growth and Development of Collagen Fibrils in Connective Tissue.*, in *Ultrastructure of the Connective Tissue Matrix*, A. Ruggeri and P.M. Motta, Editors. 1984, Martinus Nijhoff: Boston. p. 34-64.
29. Payne, B., *Unpublished Data.* .
30. Puliafito, C.A., K. Wong, and R.F. Steinert, *Quantitative and Ultrastructural Studies of Excimer Laser Ablation of the Cornea at 193 and 248 Nanometers.* Lasers in Surgery and Medicine, 1987. **7**: p. 155-9.
31. Singh, R., D. Norton, L. Laude, J. Narayan, and J. Cheung, eds. *Advanced Laser Processing of Materials-Fundamentals and Applications*. Materials Research Society. Vol. 387. 1995, Materials Research Society: Boston. 674.
32. Spripov, V.P., *Metastable Liquids*. 1974, New York: John Wiley and Sons.

33. Srinivasan, R., *Ablation of Polymers and Biological Tissue by Ultraviolet Lasers.* Science, 1986. **234**(October): p. 559-65.
34. Srinivasan, R., P.E. Dyer, and B. Braren, *Far-Ultraviolet Laser Ablation of the Cornea: Photoacoustic Studies.* Lasers in Surgery and Medicine, 1987. **6**: p. 514-519.
35. Staveteig, P.T. and J.T. Walsh, Jr., *Dynamic 193-nm optical properties of water.* Applied Optics, 1996. **35**(19): p. 3392-3403.
36. Venugopalan, V., N.S. Nishioka, and B.B. Mikic, *The Thermodynamic Response of Soft Biological Tissue to Pulsed Ultraviolet Laser Irradiation.* Biophysical Journal, 1995. **69**: p. 1259-71.
37. Venugopalan, V., N.S. Nishioka, and B.B. Mikic, *The thermodynamic response of soft biological tissues to pulsed infrared-laser irradiation.* To appear in Biophysical Journal, 1996. **70**(6).
38. Walsh, J.T., *Pulsed Laser Ablation of Tissue: Analysis of the Removal Process and Tissue Healing*, in *Medical Engineering*. 1988, Massachusetts Institute of Technology: Massachusetts. p. 312.
39. Walsh, J.T., T.F. Deutch, T.J. Flotte, M.R. Prince, and R.R. Anderson. *Comparison of Tissue Ablation by Pulsed CO_2 and Excimer Lasers.* in *Conference on Lasers and Electro-Optics*. 1986. Washington D.C: Optical Society of America.
40. Walsh, J.T., Jr. and T.F. Deutsch, *Pulsed CO_2 Laser Tissue Ablation: Measurement of the Ablation Rate.* Lasers in Surgery and Medicine, 1988. **8**: p. 264-75.
41. Walsh, J.T., Jr. and T.F. Deutsch, *Pulsed CO_2 Laser Ablation of Tissue: Effect of Mechanical Properties.* IEEE Transactions on Biomedical Engineering, 1989. **36**(12): p. 1195-1201.
42. Walsh, J.T., Jr. and T.F. Deutsch, *Measurement of Er:YAG laser Ablation Plume Dynamics.* Applied Physics B: Photophysics and Laser Chemistry, 1991. **52**: p. 217-224.
43. Weast, R.C., ed., *CRC Handbook of Chemistry and Physics*. 1985, Boca Raton: CRC Press.
44. Yamada, H., *Strength of Biological Materials*. 1973, N.Y: Robert E. Krieger. 297.
45. Yannas, I.V., *Collagen and Gelatin in a Solid State.* Journal of Macromolecular Science Revisions and Macromolecular Chemistry, 1972. **C7**: p. 49-104.
46. Zweig, A.D., *A thermo-mechanical model for laser ablation.* Journal of Applied Physics, 1991. **70**(3): p. 1684-91.